

Neuron, Volume 75

Supplemental Information

Nanoscopy of Living Brain Slices

with Low Light Levels

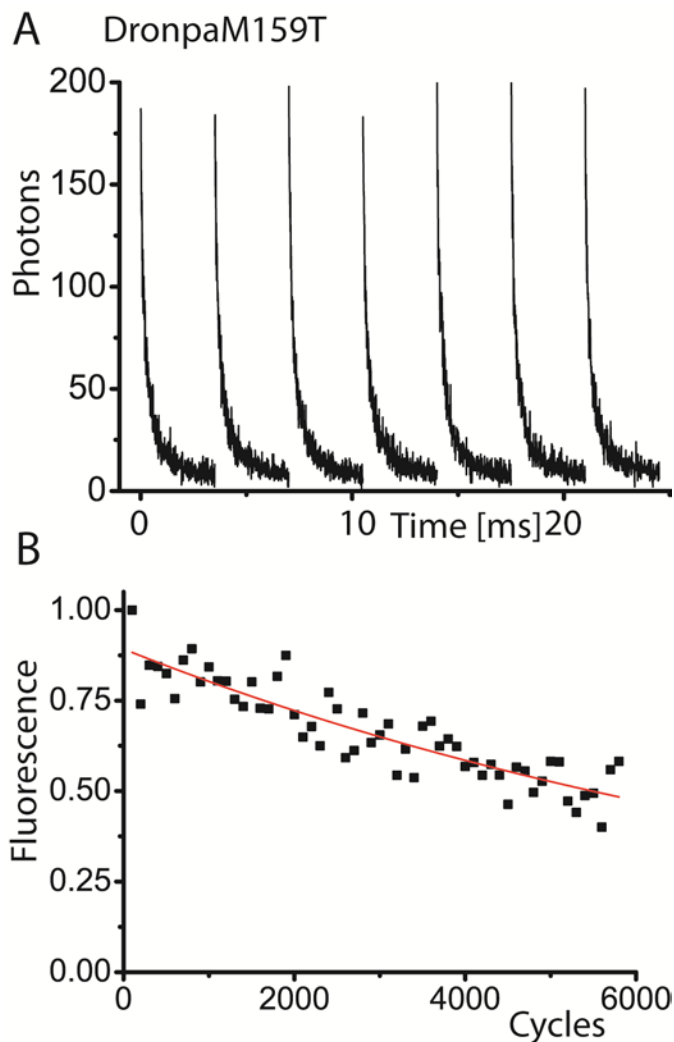
Ilaria Testa, Nicolai T. Urban, Stefan Jakobs, Christian Eggeling, Katrin I. Willig, and Stefan W. Hell

Inventory of Supplemental Information

The supplemental information contains five figures and four movies.

Figure S1. Switching behavior and photostability of Dronpa-M159T suspended in a proteinpolyacrylamide matrix (related to Figure 1)

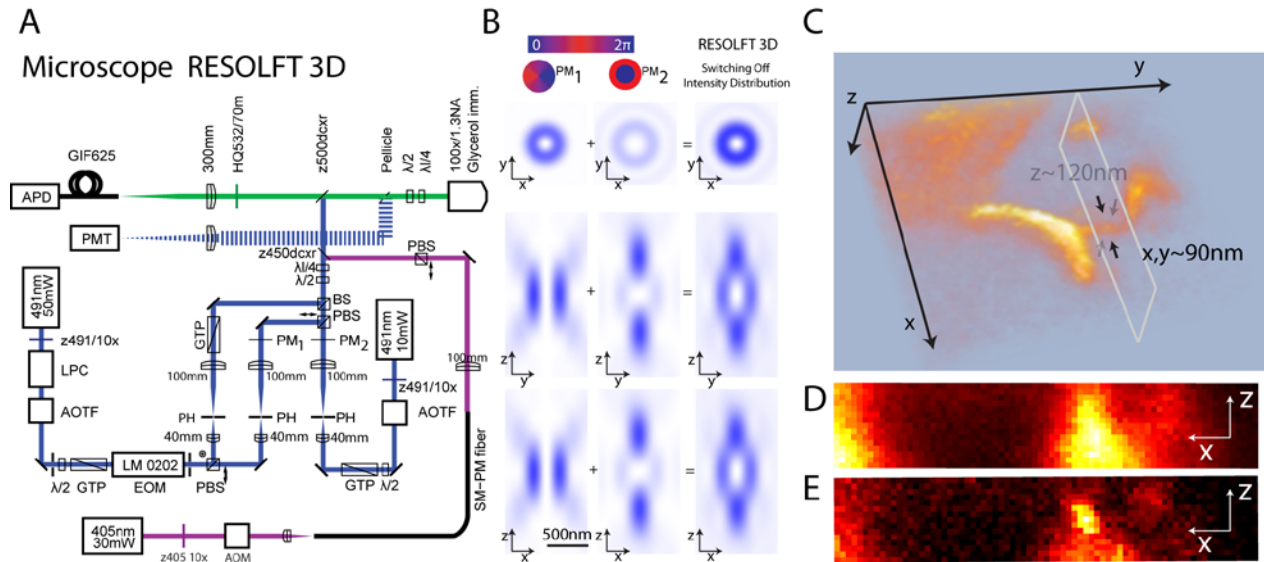
(A) Switching-off behavior of the 'negative' switching fluorophore Dronpa-M159T. Each depicted switching-off curve is the average of ten switching cycles. In each cycle the proteins were first switched into the ON-state using 405 nm laser light ($I_{405}= 2.1 \text{ kW/cm}^2$), and subsequently illuminated with 491nm laser light ($I_{491}=1.5 \text{ kW/cm}^2$), thereby switching them to the OFF-state. Dronpa-M159T displayed a switching-off half-time of 280 μs ; the switching lifetime depends, however, on the immediate molecular environment of the fluorescent protein and on the switching power used. By increasing the switching-off laser intensity from 1.5 to 6 kW/cm^2 , the halftime could be reduced from 280 μs to 100 μs . (B) Bleaching behavior of Dronpa-M159T. The proteins were switched repeatedly from the on to off state and back again, 6000 times in total. Each point in the graph represents the number of photons emitted in 100 added-up ON-OFF cycles. The data in the curve has been



background subtracted, normalized and fitted with a monoexponential decay (for clarity). The data clearly shows that, under the above intensity and timing conditions ($I_{405}= 2.1 \text{ kW/cm}^2$, $I_{491}=1.5 \text{ kW/cm}^2$), Dronpa-M159T can undergo more than 6000 ON-OFF cycles before bleaching down to <50% of the initial signal.

The protein polyacrylamide matrix was prepared as follows: 24.5 μl purified Dronpa-M159T (0.09mM) was mixed with 17.5 μl Tris-HCl pH 7.5, 30 μl acrylamide (Rotiphorese Gel 30, Roth, Karlsruhe, Germany), 0.75 μl 10 % ammonium persulfate and 1 μl 10 % TEMED. About 10 μl of this solution was pipetted onto a glass microscope slide and a cover slip was pressed onto the sample to ensure an appropriately thin layer. After complete polymerization, the sample was sealed with silicon-based glue (Picodent twinsil, Picodent, Wipperfurth, Germany) to prevent drying-out.

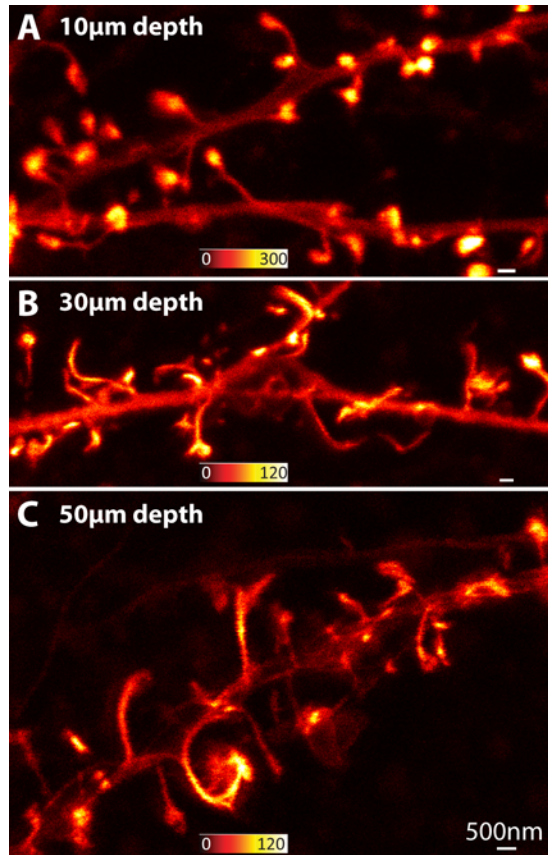
Figure S2. RESOLFT with subdiffraction resolution in three dimensions (related to Figure 2)



(A) Scheme of our home-made RESOLFT 3D microscope. LPC: laser power controller; AOTF, AOM: acousto-optic modulators; GTP: Glan-Thompson prism; EOM: electro-optic modulator (polarization rotator); PBS: polarizing beam splitter; PH: pinhole (10 μm in diameter); PM_1 : phase mask (vortex plate or phase disc), PM_2 : phase mask (annular plate); BS: 50:50 beam splitter; z491/10x, z405/10x, HQ532/70m: laser clean-up and fluorescence filters; z450dcxr, z500dcxr: dichroic mirrors; 5 mm: achromatic lenses with respective focal lengths; $\lambda/2$, $\lambda/4$: retardation plates; APD: avalanche photodiode; PMT: photomultiplier tube; SM-PM fiber: single-mode polarization-maintaining fiber; GIF625: gradient-index multi-mode fiber with 62.5 μm core diameter, acting as confocal pinhole.

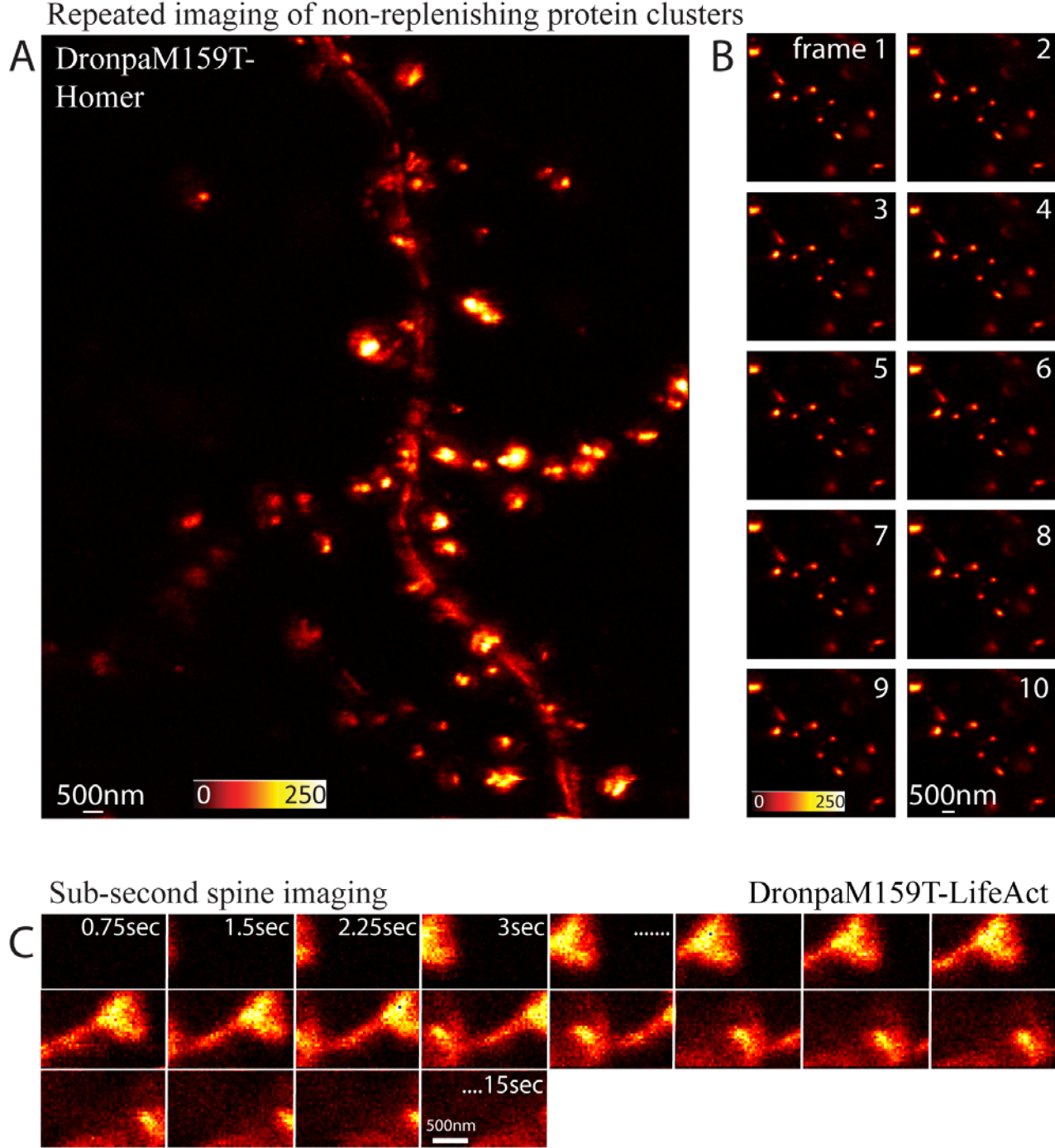
(B) Calculated focal intensity distributions for a beam passing through the phase masks PM_1 , PM_2 and the sum of both. PM_1 creates an xy -doughnut, PM_2 a z -doughnut. The combination of both intensity distributions is used in the RESOLFT-3D experiments to switch off fluorescent proteins in the xy -plane as well as along the optical (z -) axis, so in the entire periphery of the focal volume. (C) 3D reconstruction of two dendritic spines convoluted in three dimensions. The image comprises 15 optical sections, each $4 \times 3 \mu\text{m}^2$ (in xy) and taken every 60 nm along the optical (z -) axis. The three dimensional resolution can be seen clearly, when viewed along the xz -plane (gray box in C): in contrast to the confocal image (D) the separation of both spine necks can be clearly distinguished in RESOLFT-3D mode (E). Six consecutive xz -slices were summed up to create the printed xz -frames D,E.

Figure S3. RESOLFT imaging at various depths inside the living brain slices (related to Figure 3)



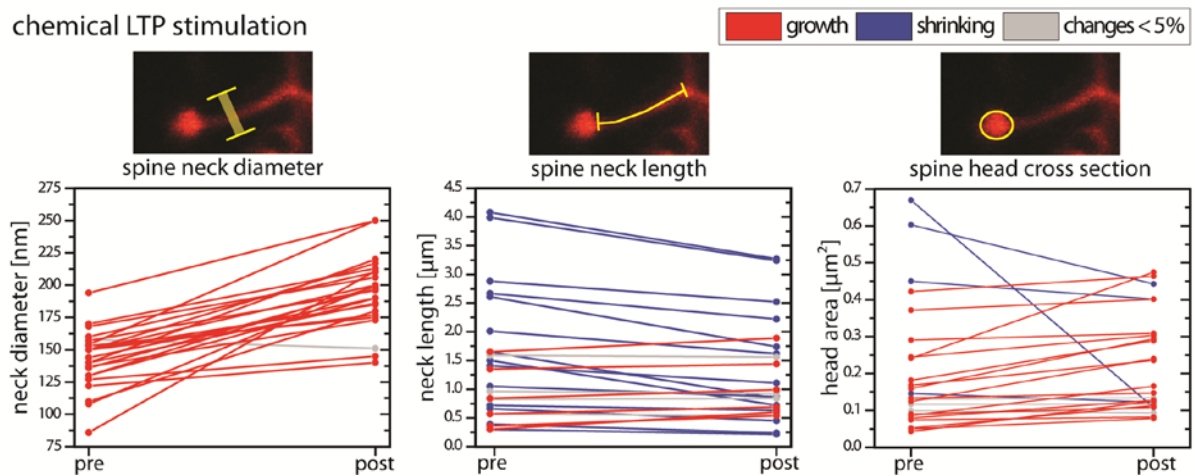
By adjusting the correction collar of our objective lens (between a value of 5.5 and 7) to counteract the aberrations occurring at various imaging depths, we were able to acquire RESOLFT images at different depths within the brain sample; here, at (A) 10, (B) 30 and (C) 50 μm inside living brain slices, respectively. Over this entire range we did not observe any image degradation in terms of signal or resolution impairment. The pixel size in (A) was 30 nm, and in (B) and (C) 25 nm. Scale bar is 500 nm.

Figure S4. RESOLFT imaging of small neuronal structures: repeated imaging of non-replenishing switchable fluorescent protein labels (RSFP). Sub-second imaging of single dendritic spines (both related to Figure 4)



(A,B) We expressed a fusion protein of Dronpa-M159T^{v2.0} with Homer1c(Inoue et al., 2007; Xiao et al., 1998), a scaffolding protein of the postsynaptic density (also termed Ves1-1L or PSD-Zip45), in living hippocampal brain slices. For this purpose, we produced a new Semliki Forest Virus by replacing the Lifeact coding sequence with the sequence for Dronpa-M159T^{v2.0}-Homer1c (courtesy of Anita Aperia and Alexander Bondar of the Karolinska Institute, Stockholm) in the pSCA3 vector. Unlike the Lifeact label, this label cannot be replenished quickly, leaving these structures more prone to bleaching influences. (A) In an overview picture (19.5x19.5 μm^2 , pixel size 30nm, 5 optical sections) the Homer1c protein can be seen to cluster in spots of various sizes along the dendritic shaft. (B) Repeated imaging of a smaller area (6.6x6.6 μm^2 , pixel size 30nm, no z-projection) displays only marginal bleaching after ten frames, despite the label not being able to replenish during the imaging. The lookup table is identical for all images. We repeated this imaging scheme at different locations for up to 100 frames, observing 50% bleaching after about 40 frames. The images in B) were deconvolved using a Richardson-Lucy algorithm enhancing contrast. (C) Sub-second RESOLFT imaging of a single dendritic spine labeled with Lifeact-Dronpa-M159T^{v2.0}. A series of twenty frames (1.75x0.9 μm^2 , pixel size 35nm, pixel dwell-time 500 μs) was recorded by automatically translating the stage in 200 nm steps along the x-direction in between each frame, mimicking a movement of the spine through the field of view. Each frame was recorded in 0.75 seconds. The experiment shows the ability of RESOLFT nanoscopy to record specimen movements on the subsecond time scale.

Figure S5. Quantitative evaluation of the morphological parameters of dendritic spines before and after LTP stimulation (related to Figure 5)



We analyzed the morphology of 24 dendritic spines from two different brain slices before and after LTP stimulation. All increases are denoted in red, all decreases in blue, and all cases with little to no visible changes in dimension are marked in grey. (A) Spine neck widths were measured by determining the FWHMs of 3-pixel-wide line intensity profiles taken from the same position before and after stimulation. (B) The length of the spine neck were measured from the spine base anchored to the dendritic shaft up to the beginning of the spine head. (C) The area, or cross section, of the spine heads was determined by drawing a bounding box around all pixels over a certain threshold in the spine head and determining the resulting surface area. All these analyses were performed with Image J.

On RESOLFT imaging speed:

The resolution of a microscope is the ability to separate (an arbitrary number of) adjacent (fluorescent) features in space. Diffraction only precludes the separation of adjacent features that are closer together than ~ 250 nm, i.e. half the wavelength of light; features that are further apart than this distance (within the field of view) can be separated. Therefore, the ability to overcome the diffraction barrier is equivalent to being able to separate features falling within the 'diffraction range' of 250 nm extent. All current superresolution methods (of significant practical relevance) separate the fluorescent features falling within this range by preparing them so that they fluoresce sequentially. To this end they keep most (or all) of the fluorophores residing within the diffraction range in a fluorescence OFF state while allowing just a few or just a single fluorophore to assume the fluorescent ON state. Making sure that fluorophores of nearby features assume the ON-state sequentially in time, allows adjacent features/fluorophores to be registered sequentially and hence to be separated. The superresolution methods broadly fall into two categories, depending on how the ON state is prepared in space.

1] Coordinate-targeted: the on-state is predetermined with a light pattern. This is the case in the STED and RESOLFT method. The resolution is determined by the number of photons inducing the ON-OFF transition.

2] Stochastic: the fluorophores are turned on individually, molecule by molecule, while all other fluorophores have to reside in the OFF state. This is the case in STORM, PALM, etc. The resolution is determined by the number m (typically > 100) of photons detected from the single emitter.

Methods of category 1 (STED/RESOLFT) are generally faster at reading out the molecules within the critical 250 nm diffraction range, because they need not reading out the molecules individually; they simultaneously collect photons from *all* (usually several) fluorophores residing within a range given by the $d \ll 250$ nm. The latter is predetermined by the beam of light applied to keep fluorophores in the OFF state. Moreover, since the role of the fluorescent photons is just to indicate the sheer presence of the fluorescent feature, they require much fewer detected photons from feature and fluorescent molecule. This is because the feature position is predefined by the beam inducing the ON/OFF transition, i.e by the number of the photons in the beam (inducing the transition) and the location of its zero.

In the case of RESOLFT, the speed limit of reading out the 250 nm zone is essentially given by the pixel size (given by $d/2$ following the Nyquist criterion) and the switching kinetics of the proteins at the applied

intensities, defining the average time the fluorophore requires to assume the other state. For the proteins used here, this is of the order of 100 μ s, which is the physical limit of the recording speed. This physical limit can be reduced by resorting to/developing fluorescent proteins with even faster switching kinetics. For a spatial resolution $d = 50$ nm, the Nyquist criterion requires a pixel size of 25 nm, meaning that the typical diffraction zone of 250 nm entails 100 pixels, which can then be read out in 10 ms or 40 ms, for a 100 μ s and 400 μ s pixel dwell time, respectively. These recording times yield 25-100 frames per second as the speed limit of the RESOLFT concept using these probes.

Supplemental References

Inoue, Y., Udo, H., Inokuchi, K., and Sugiyama, H. (2007). Homer1a regulates the activity-induced remodeling of synaptic structures in cultured hippocampal neurons. *Neuroscience* *150*, 841-852.

Xiao, B., Tu, J.C., Petralia, R.S., Yuan, J.P., Doan, A., Breder, C.D., Ruggiero, A., Lanahan, A.A., Wenthold, R.J., and Worley, P.F. (1998). Homer Regulates the Association of Group 1 Metabotropic Glutamate Receptors with Multivalent Complexes of Homer-Related, Synaptic Proteins. *Neuron* *21*, 707-716.

Movie S1. Rotational movie of the 3D-RESOLFT reconstruction shown in Figure 2D (related to Figure 2)

The movie shows two separate dendritic spines labeled with Lifeact-Dronpa-M159T. Both spines show high concentrations of actin, but from one spine, an actin filament extends from the base of the spine neck along the edge of the dendritic shaft. The field of view was $4 \times 6 \times 1.2 \mu\text{m}^3$.

Movie S2. Rotational movie of a 3D reconstruction depicting a region of spiny dendrite (related to Figure 2)

The movie shows the 3D reconstruction of a dendrite region, first recorded in the confocal mode, then using 3D-RESOLFT. The dendrite was located $35 \mu\text{m}$ deep inside the brain slice and was labeled with Lifeact-Dronpa-M159T. The field of view was $5.9 \times 6.4 \times 3.6 \mu\text{m}^3$, and the voxel size was $50 \times 50 \times 60 \text{ nm}^3$.

Movie S3. Rapid time-lapse RESOLFT imaging of dendritic spines, as described in Figure 4A (related to Figure 4)

The movie shows three independent time-lapse image series (from top to bottom), each consisting of 40 frames, recorded at 7 s / frame and displayed at 8 frames/s . The left side displays the raw data, with the corresponding deconvolved images on the right. The spines in the time-lapse series are in a state of constant, subtle flux shifting positions, drifting slowly in and out of focus and some undergoing slow, minute morphological changes.

Movie S4. Continuous RESOLFT imaging of spontaneous actin rearrangements in a spiny dendrite, as described in Figure 4B. (related to Figure 4)

A stretch of spiny dendrite was imaged continuously for two hours, revealing a series of extensive movements and morphological changes that occurred during that time frame. Each frame depicts 15min, displayed in the movie at 1 frame/second .